

# Integrability vs. non-integrability

*hard hexagons and hard squares compared*

Barry M. McCoy

CN Yang Institute of Theoretical Physics

State University of New York,

Stony Brook, NY, USA

In collaboration with

**Michael Assis**, Stony Brook University

**Jesper Jacobsen**, ENS Paris

**Iwan Jensen**, University of Melbourne

**Jean-Marie Maillard**, University of Paris VI

Based in part on arXiv: 1406XXX

## General motivation

There is a fundamental paradox in the practice of theoretical physics. We do exact computations on integrable systems which have very special properties and then apply the intuition gained to real generic systems which have none of the special properties which allowed the exact computations to be carried out. The ability to do exact computations relies on the existence of sufficient symmetries which allow the system to be solved by algebraic methods. Generic systems do not possess such an algebra and the distinction between integrable and non-integrable may be thought of as the distinction of algebra versus analysis.

## Specific motivation

1) The discovery in 1999 by Nickel that the Ising susceptibility has a natural boundary as a function of temperature.

2) The discovery in 2005 by Fendley, Schoutens and van Ereteen that at  $z = -1$  all the eigenvalues of the transfer matrix for hard squares are roots of unity.

Neither of these phenomenon is explained by the renormalization group or field theory methods and neither are seen in series expansions or in exactly solved models.

# Outline

1. Preliminaries
2. Partition function zeros
3. Transfer matrix equimodular curves
4. Behavior on the negative fugacity axis
5. Universality and analyticity
6. Conclusion

# 1. Preliminaries

The hard square (hexagon) lattice gas is defined by a (occupation) variable  $\sigma = 0, 1$  at each site of a square (triangular) lattice with the restriction that no two adjacent sites can have the values  $\sigma = 1$  (ie. the gas has nearest neighbor exclusion). Calling  $g(n; L_v, L_h)$  the number of such configurations which has  $n$  occupied sites the grand partition function on the finite  $L_v \times L_h$  lattice is defined as the polynomial

$$Z_{L_v, L_h}(z) = \sum_{n=0} z^n g(n; L_v, L_h)$$

These polynomials can be characterized by their zeros  $z_j$  as

$$Z_{L_v, L_h}(z) = \prod_j (1 - z/z_j)$$

where the  $z_j$  and the degree of the polynomial will depend on the lattice boundary conditions.

## Physical free energy

The physical free energy is defined for real positive values of the fugacity  $z$  by the limit

$$F = \lim_{L_v, L_h \rightarrow \infty} (L_v L_h)^{-1} \ln Z_{L_v, L_h}(z)$$

This limit must be independent boundary conditions and the aspect ratio  $L_v/L_h$  for thermodynamics to hold. For values of  $z$  not on the positive  $z$  axis the physical free energy is defined by analytic continuation into the zero free regions which include the positive  $z$  axis. There is no general theorem concerning further continuation beyond the zero free region. It is important to note that **analytic continuation does not commute with the thermodynamic limit.**

## Historical review

The free energy for both hard squares and hexagons has been studied by series methods since the 1960's. These studies find two singularities:

For hard squares:

$$z_c = 3.79625517391234(4) \quad z_d = -0.119338886(5)$$

For hard hexagons:

$$z_c = 11.09016 \dots \quad z_d = -0.09016 \dots$$

The singularity at  $z_d$  determines the radius of convergence and at  $z_c$  there is a phase transition to an ordered state. In 1980 Baxter computed the hard hexagon physical free energy exactly for both high and low density and found that the **only** singularities are at infinity and

$$z_c = \frac{11+5\sqrt{5}}{2} \quad z_d = \frac{11-5\sqrt{5}}{2}.$$



## 2. Partition function zeros

For both hard squares and hard hexagons we consider three separate partition functions for three separate boundary conditions for  $L_v \times L_h$  lattices:

1. Toroidal:  $Z_{L_v, L_h}^{CC}(z)$

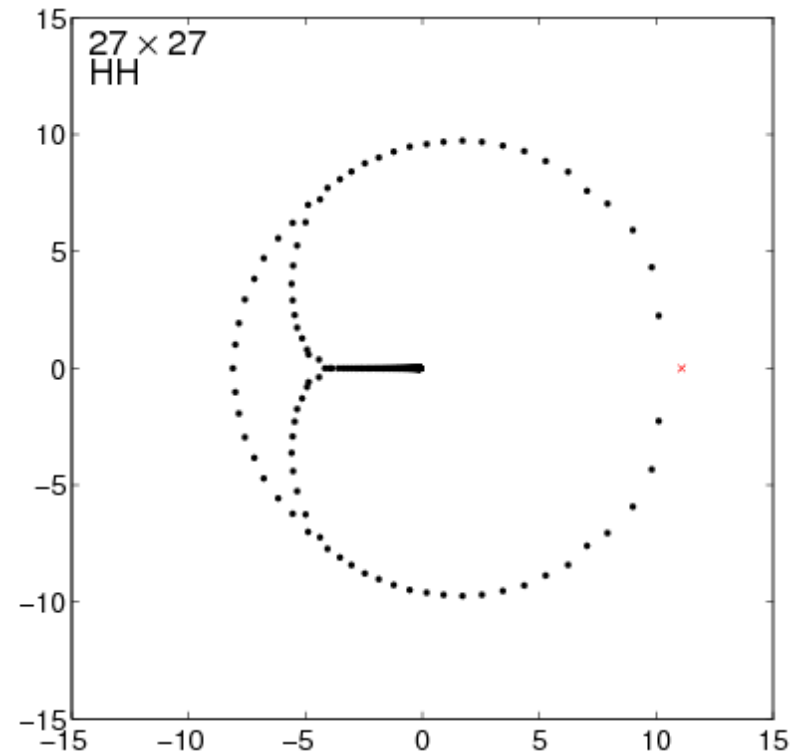
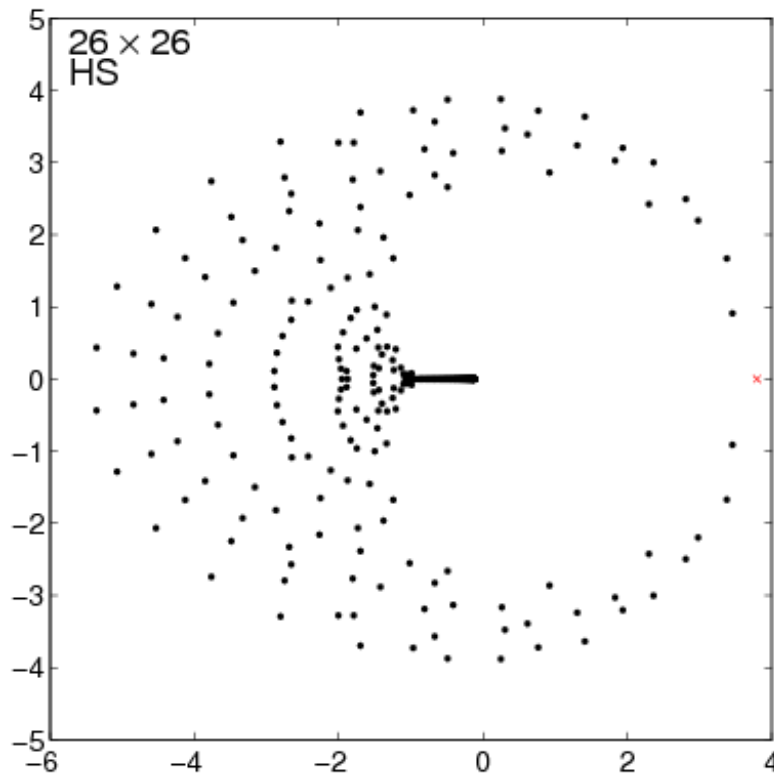
2. Cylindrical in one direction:  $Z_{L_v, L_h}^{CF}(z)$ ,  $Z_{L_v, L_h}^{FC}(z)$

3. Free:  $Z_{L_v, L_h}^{FF}(z)$

For  $L_h = L_v = L$  we have

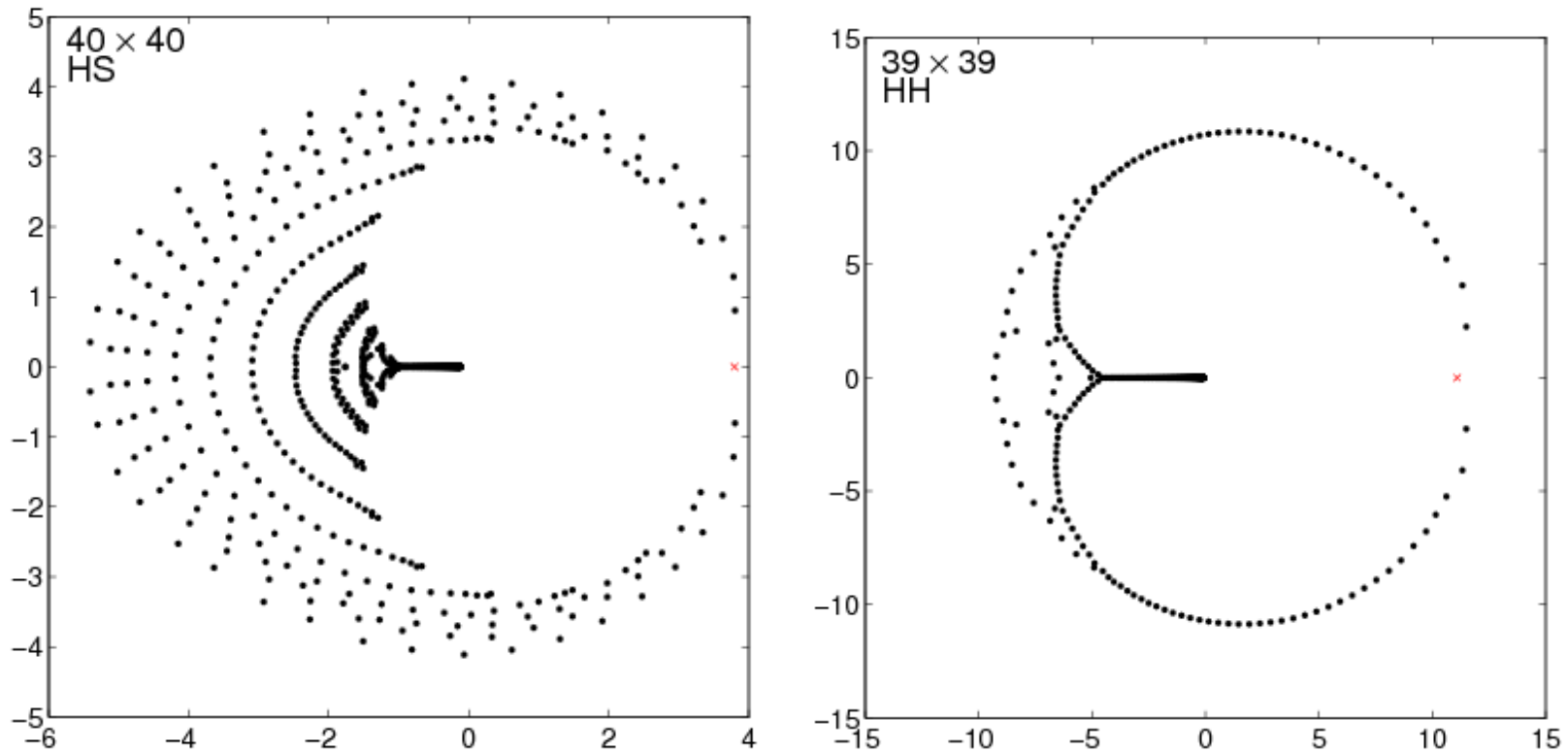
$$Z_{L, L}^{CF}(z) = Z_{L, L}^{FC}(z)$$

## Toroidal boundary conditions



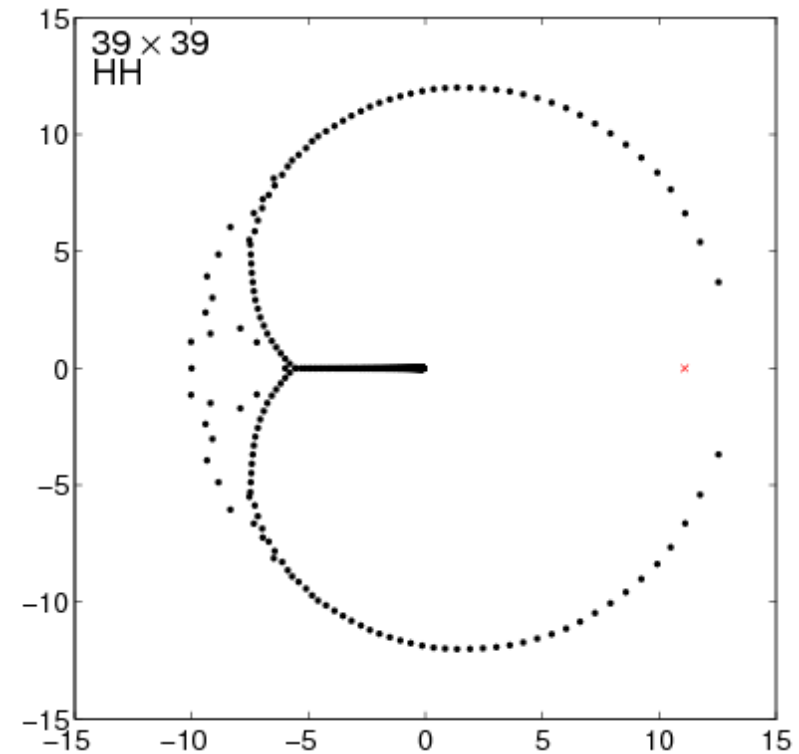
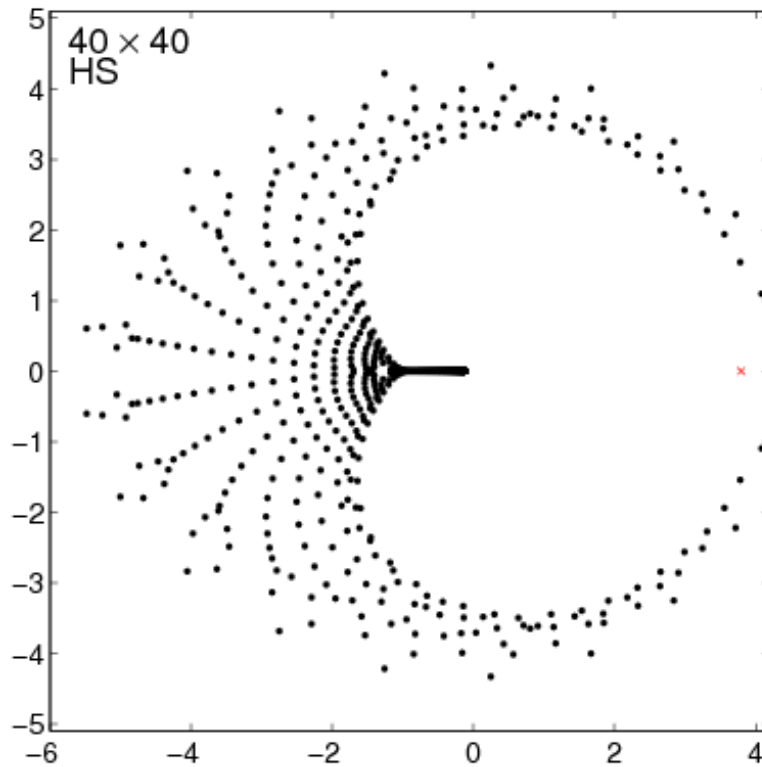
The zeros of the partition function  $Z_{L,L}^{CC}(z)$  with toroidal boundary conditions of hard squares for the  $26 \times 26$  lattice on the left vs. hard hexagons for the  $27 \times 27$  lattice on the right. The red cross is  $z_c$ .

## Cylindrical boundary conditions



The zeros of the partition function  $Z_{L,L}^{FC}(z) = Z_{L,L}^{CF}(z)$  with cylindrical boundary conditions of hard squares for the  $40 \times 40$  lattice on the left vs. hard hexagons for the  $39 \times 39$  lattice on the right. The red cross is  $z_c$ .

## Free boundary conditions



The zeros of the partition function  $Z_{L,L}^{FF}(z)$  with free boundary conditions of hard squares for the  $40 \times 40$  lattice the left vs. hard hexagons for the  $39 \times 30$  lattice on the right. The red cross is  $z_c$ .

## Discussion for hexagons

1. For hard hexagons the zeros for all three sets of boundary conditions are qualitatively the same. They lie on a few well defined sets of curves.
2. In the thermodynamic limit the zeros pinch the  $z$  axis at  $z_c = (11 + 5\sqrt{5})/2$ .
3. We know from Baxter that the **only** places on the curve of zeros where the density the low and high density phases have singularities are  $z_c$  and  $z_d$ . There are **no** other singularities on the curves of zeros and density in **both** the low and high density phases can be analytically continued **beyond** the zero free region to the entire  $z$  plane.

## Discussion for squares 1

1. The zeros of hard squares are seen to lie in an area.
2. For cylindrical boundary conditions the filling up of this area proceeds in a remarkable regular fashion.

For the lattices  $4N \times 4N$  there are  $N - 1$  outer arcs each of  $4N$  points, then there is a narrow arclike area with close to  $4N$  zeros and finally there is an inner structure that is connected to  $z = -1$ . For the innermost of the  $N - 1$  arcs the zeros appear in well defined pairs.

For lattices  $(4N + 2) \times (4N + 2)$  there are  $N - 1$  outer arcs each of  $4N + 2$  points, then a narrow arclike area which has close to  $4N + 2$  zeros and finally an inner structure that is connected to  $z = -1$ .

## Discussion for squares 2

3. The structure of arcs appears to converge in the  $L \rightarrow \infty$  limit to a **wedge which hits the positive  $z$  axis at  $z_c$** . This is distinctly different from the behavior of hard hexagons. Series expansions confirm that the leading singularity at  $z_c$  is the same as the Ising model. Will a wedge behavior of the zeros produce further singularities at  $z_c$  **not** seen in Ising?

4. It is **unknown** if in the thermodynamic limit there is a singularity at  $z = -1$  or if analytic continuation beyond the zero free region is possible.

### Discussion for squares 3.

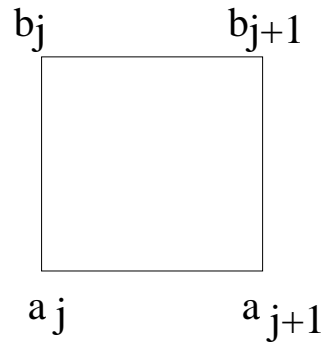
5. A combined plot of hard square zeros of  $Z_{L,L}^{CF}(z) = Z_{L,L}^{FC}(z)$  for the  $L \times L$  lattice with cylindrical boundary conditions for  $12 \leq L \leq 40$ . exhibits a mod six effect. There is a distinguished curve where only points  $L = 6n + 4$  lie.

6. Unlike hard hexagons the zeros of  $Z_{L,L}^{FF}(z)$  are qualitatively different from  $Z_{L,L}^{CF}(z)$



### 3. Transfer matrix equimodular curves

The partition function may also be described by transfer matrices obtained from local Boltzmann weights



**For hard squares:**

$$W(a_j, a_{j+1}; b_j, b_{j+1}) = 0 \text{ for } a_j a_{j+1} = a_{j+1} b_{j+1} = b_j b_{j+1} = a_j b_j = 1$$

$$\text{and otherwise } W(a_j, a_{j+1}; b_j, b_{j+1}) = z^{b_j}$$

**For hard hexagons** we also have

$$W(a_j, a_{j+1}; b_j, b_{j+1}) = 0 \text{ for } a_{j+1} b_j = 1$$

## Transfer matrices

The transfer matrix  $T_C(z; L_h)$  for cylindrical boundary conditions has matrix elements

$$T_{C\{b\},\{a\}}(z; L_h) = \prod_{j=1}^{L_h} W(a_j, a_{j+1}; b_j, b_{j+1}).$$

The transfer matrix  $T_F(z; L_h)$  for free boundary conditions is

$$T_{F\{b\},\{a\}}(z; L_h) = \left( \prod_{j=1}^{L_h-2} W(a_j, a_{j+1}; b_j, b_{j+1}) \right) W_F(a_{L_h-1}, a_{L_h}; b_{L_h-1}, b_{L_h})$$

where

$$W_F(a_{L_h-1}, a_{L_h}; b_{L_h-1}, b_{L_h}) = z^{b_{L_h-1} + b_{L_h}}.$$

## Partition functions

The partition functions are obtained from the transfer matrices as

$$Z_{L_v, L_h}^{CC}(z) = \text{Tr} T_C^{L_v}(z; L_h).$$

$$Z_{L_v, L_h}^{CF}(z) = \text{Tr} T_F^{L_v}(z; L_h),$$

$$Z_{L_v, L_h}^{FC}(z) = \langle \mathbf{v}_B | T_C^{L_v-1}(z; L_h) | \mathbf{v}'_B \rangle,$$

$$Z_{L_v, L_h}^{FF}(z) = \langle \mathbf{v}_B | T_F^{L_v-1}(z; L_h) | \mathbf{v}'_B \rangle,$$

with

$$\mathbf{v}_B(a_1, a_2, \dots, a_{L_h}) = \prod_{j=1}^{L_h} z^{a_j}$$

$$\mathbf{v}'_B(b_1, b_2, \dots, b_{L_h}) = 1$$

In terms of the eigenvalues  $\lambda_k$  and eigenvectors  $\mathbf{v}_k$

$$Z_{L_v, L_h}^{CC}(z) = \sum_k \lambda_{k;C}^{L_v}(z; L_h)$$

$$Z_{L_v, L_h}^{CF}(z) = \sum_k \lambda_{k;F}^{L_v}(z; L_h)$$

$$Z_{L_v, L_h}^{FC}(z) = \sum_k \lambda_{k;C}^{L_v-1}(z; L_h) \cdot d_{C,k}$$

where  $d_{C,k} = (\mathbf{v}_B \cdot \mathbf{v}_{C,k})(\mathbf{v}_{C,k} \cdot \mathbf{v}'_B)$

$$Z_{L_v, L_h}^{FF}(z) = \sum_k \lambda_{k;F}^{L_v-1}(z; L_h) \cdot d_{F,k}$$

where  $d_{F,k} = (\mathbf{v}_B \cdot \mathbf{v}_{F,k})(\mathbf{v}_{F,k} \cdot \mathbf{v}'_B)$

## Symmetries

For both hard hexagons and hard squares the transfer matrix  $T_C(z; L_h)$  is invariant under translations and reflections and therefore momentum  $P$  and parity  $\pm$  are good quantum numbers. Furthermore the boundary vectors  $\mathbf{v}_B$  and  $\mathbf{v}'_B$  are invariant under translation and reflection. Consequently the scalar products  $(\mathbf{v}_B \cdot \mathbf{v}_{C,k})$  and  $(\mathbf{v}_{C,k} \cdot \mathbf{v}'_B)$  vanish unless  $\mathbf{v}_{C,k}$  lies in the sector positive parity  $P = 0^+$ .

For hard squares  $T_F(z; L_h)$  is invariant under reflection so the eigenvectors in the scalar products are restricted to positive parity states. However, for hard hexagons  $T_F(z; L_h)$  is not reflection invariant and all eigenvectors contribute.

## Equimodular curves and partition zeros

In the limit  $L_v \rightarrow \infty$  with  $L_h$  fixed the partition functions will have zeros on the curves where two (or more) eigenvalues have equal modulus

$$|\lambda_1(z; L_h)| = |\lambda_2(z; L_h)|$$

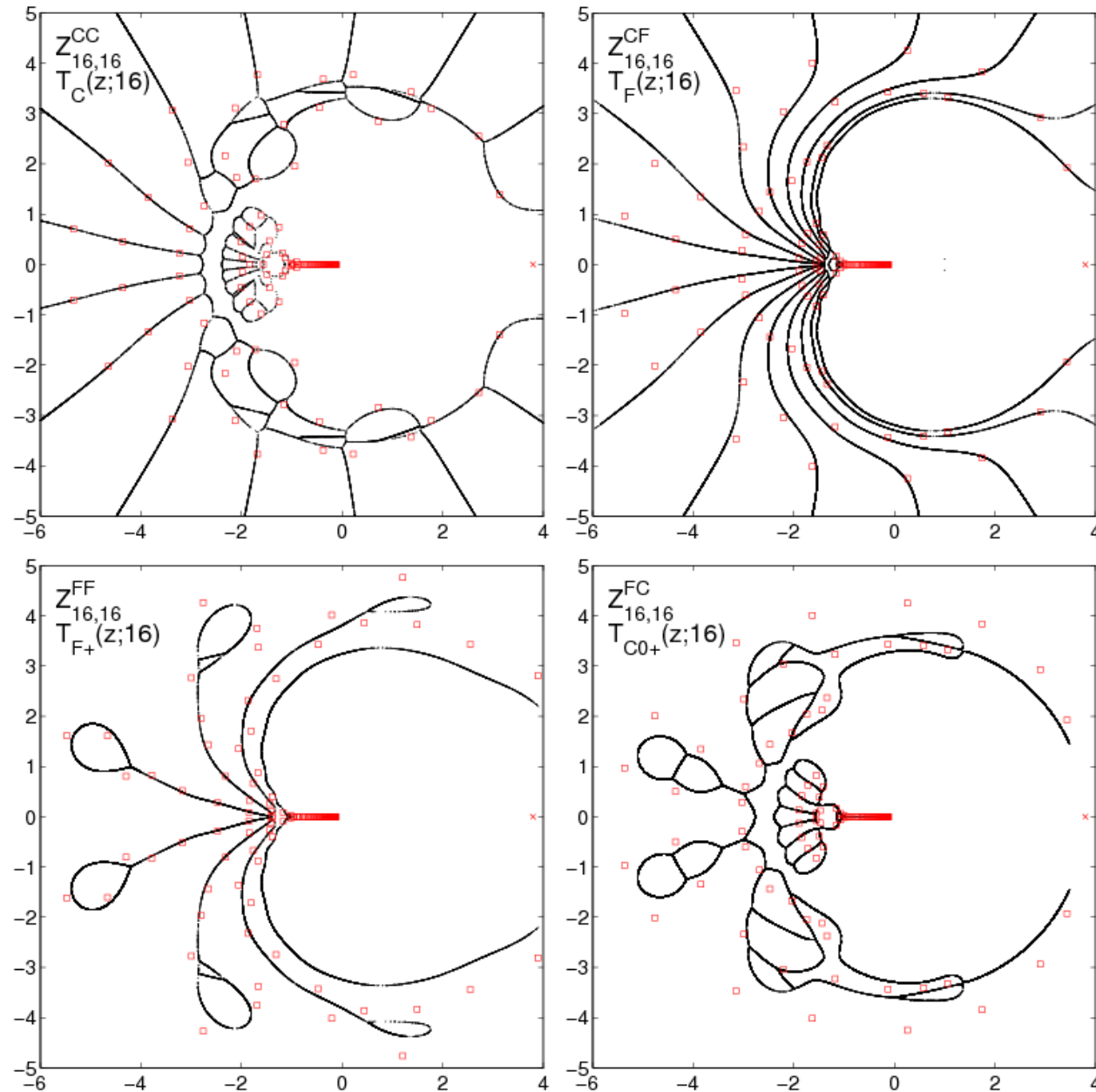
On this curve  $\lambda_1/\lambda_2 = e^{i\theta}$  with  $\theta$  real and for  $L_v$  large  $Z_{L_v, L_h}(z)$  will have a zero close to the points where  $e^{-\theta L_v} = -1$ . If we define  $s(z)$  as the arclength along the curve at the point  $z$  and define the density of zeros as

$$D(s) = \lim_{L_v \rightarrow \infty} \frac{1}{L_v (s(z_{i+1}) - s(z_i))}$$

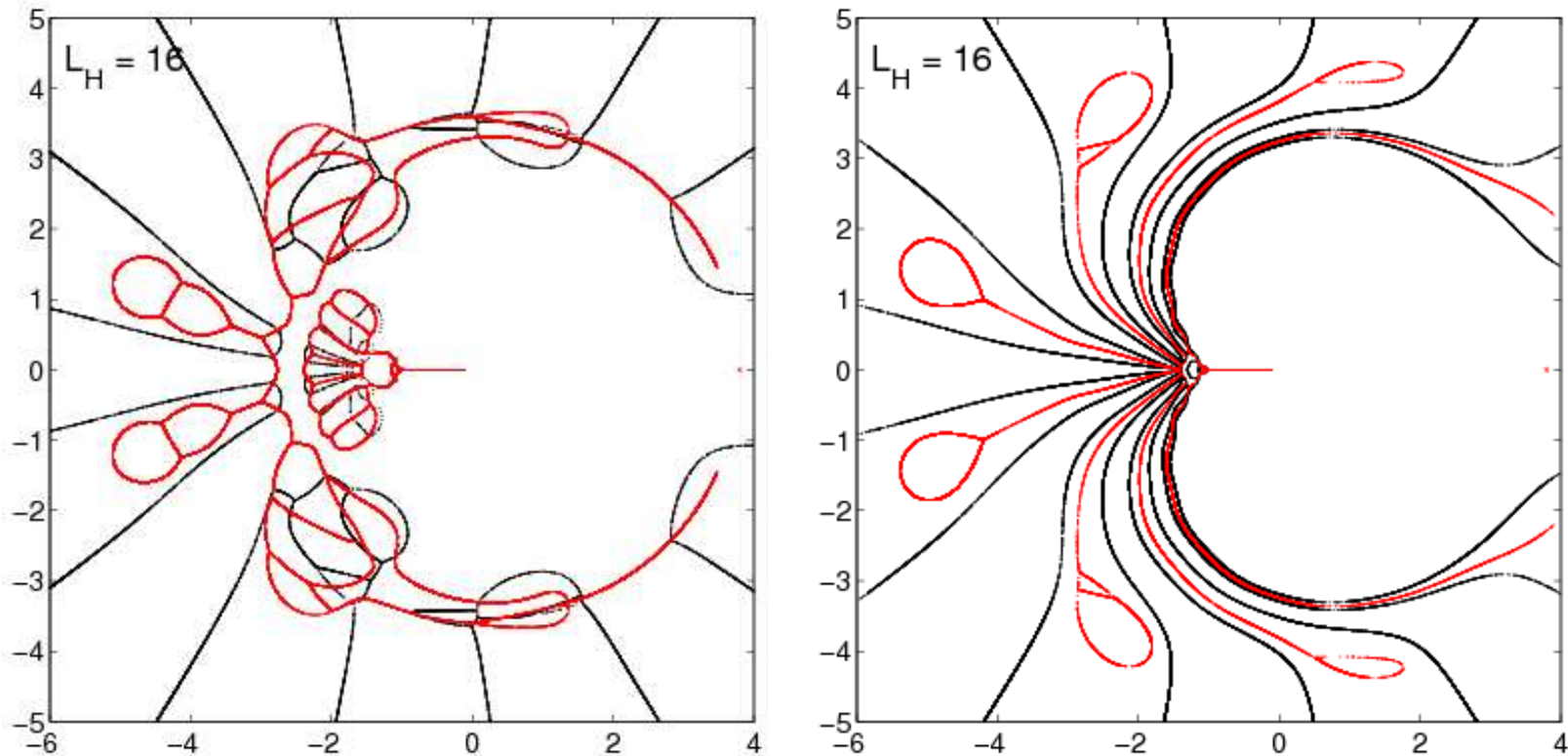
we have

$$2\pi D(s) = \lim_{L_v \rightarrow \infty} \frac{\theta(s(z_{i+1})) - \theta(s(z_i))}{s(z_{i+1}) - s(z_i)}$$

# Hard square equimodular curves vs partition function zeros for $16 \times 16$ lattices.



# Comparison of hard square equimodular curves for $L_h = 16$



On the left the equimodular curves of  $T_C(z; L_h)$  in black with the restriction to  $P = 0^+$  in red. On the right the equimodular curves of  $T_F(z; L_h)$  in black with the restriction to the positive parity sector in red.



## Hard square discussion

For hard squares there are **four** different sets of equimodular curves

$$T_C(z), T_F(z), T_{C0+}, T_{F+}(z)$$

but there are only **three** different sets of partition function zeros because for  $L_v = L_h = L$  of the identity  $Z_{L,L}^{CF}(z) = Z_{L,L}^{FC}(z)$ .

This partition function is described by both  $T_F(z)$  and  $T_{C0+}$  and the figure shows that these curves are **dramatically** different.

The curves of  $T_F$  are by far the simplest of the four curves and are in a beautiful 1-to-1 match with the arclike structure of the zeros.

The small circles in the  $T_F$  curve also match well with the circles seen in  $Z_{L,L}^{FF}(z)$ .

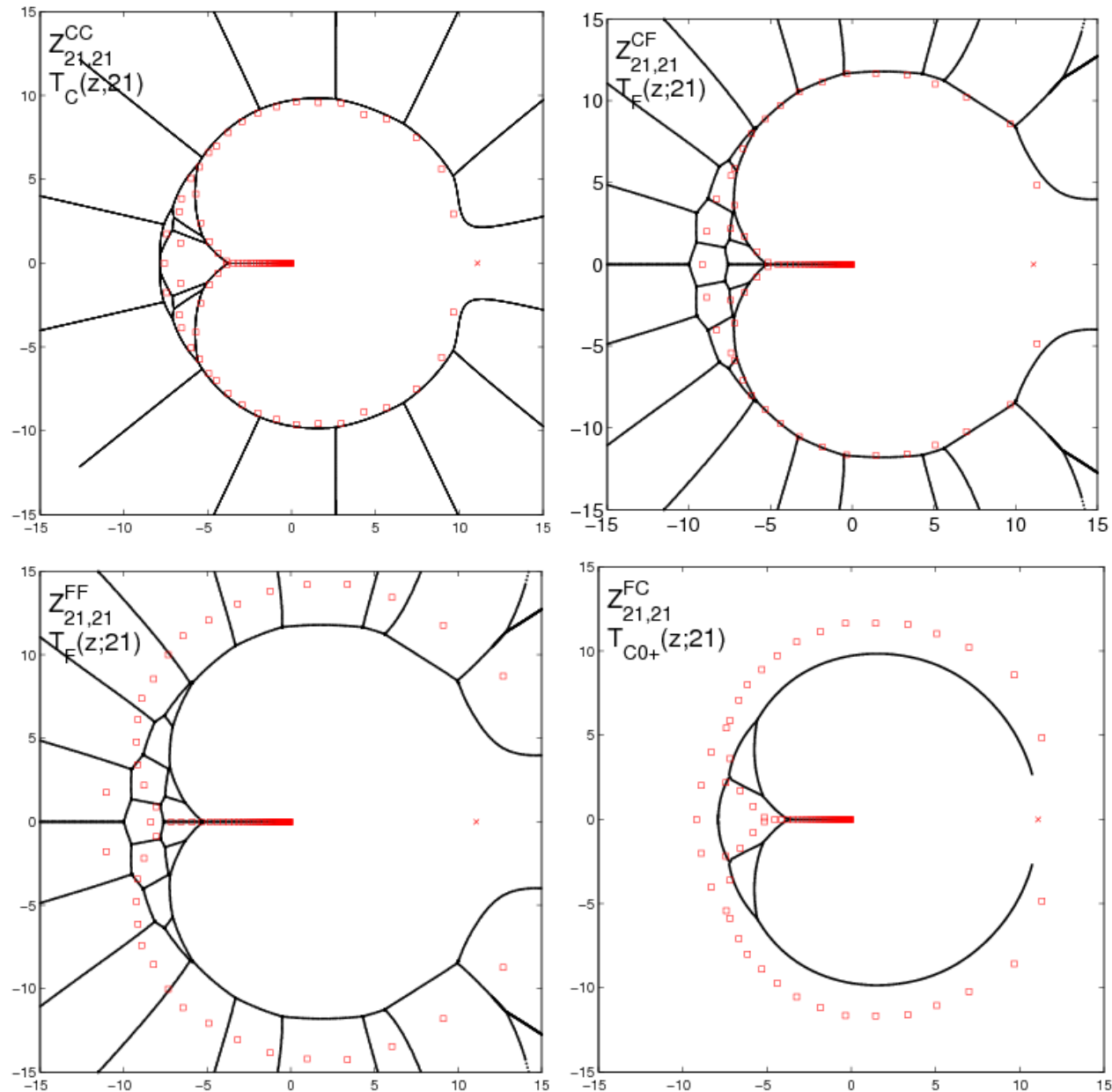
## Hard hexagons

In contrast with hard squares there are only three sets of equimodular curves:

$T_C$ ,  $T_{C0+}$  which were computed by us previously (J. Phys. A 46 (2013) 445202)

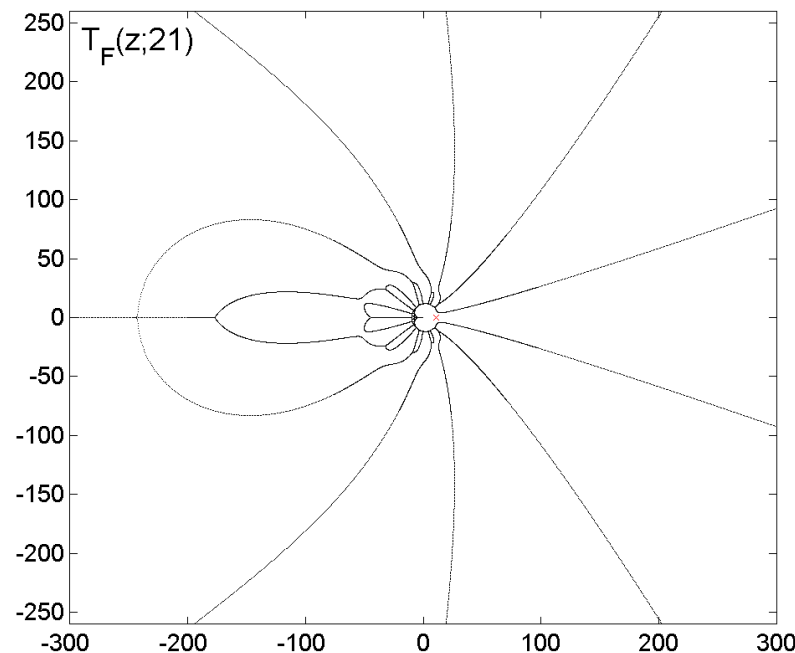
$T_F$  was not previously considered.

# Hard hexagon equimodular curves vs partition function zeros for $21 \times 21$ lattices.



## Equimodular curves for large $|z|$

There are no partition function zeros for large  $z$  and the equimodular curves which extend to infinity for  $T_C$  and  $T_F$  come from asymptotically degenerate eigenvalues in the ordered phase. For hard squares there are  $L_h$  rays for  $T_C$  and  $T_F$ . For hard hexagons there are  $2L_h/3$  rays for  $T_C$ . For hard hexagons for  $T_F$  we have



## 4. Behavior for $z \leq z_d$

Integrability conjecture for hard hexagons for  $T_F$ .

On the segment  $z \leq z_d$  we previously discovered that for hard squares there is an unbroken line segment which is an equimodular curve. On this segment the discriminant of the characteristic polynomial of  $T_C$  has only double roots where the equimodular eigenvalues are both real and equal. This is a non-generic and a property of integrability. We have found that this also holds for  $T_F$ . This strongly suggests **the conjecture that  $T_F$  has the same integrability properties that  $T_C$  has.**

## Real gaps for hard squares

In distinct contrast to hard hexagons, hard squares has segments of  $-1 \leq z \leq z_d$  where the maximum eigenvalue of both  $T_C$  and  $T_F$  is real and non degenerate. Gaps exist for all cases studied. For  $T_C$  and  $L_h \leq 14$

$L_h$	$z_l(L_h)$	$z_r(L_h)$	gap	eigenvalue sign
6	-0.52385422	-0.47481121	$4.904301 \times 10^{-2}$	-
8	-0.30605227	-0.30360084	$2.35243 \times 10^{-3}$	-
10	-0.23737268	-0.23720002	$1.7266 \times 10^{-4}$	-
	-0.77929238	-0.73645527	$4.283711 \times 10^{-2}$	+
12	-0.20401756	-0.20400239	$1.517 \times 10^{-5}$	-
	-0.49539291	-0.49352002	$1.87289 \times 10^{-3}$	+
14	-0.18464415	-0.18464265	$1.50 \times 10^{-6}$	-
	-0.37193269	-0.37180394	$1.2875 \times 10^{-4}$	+
	-0.92551046	-0.91949326	$6.01721 \times 10^{-3}$	-

## Real gaps for hard squares

Similarly for  $T_F$

$L_h$	$z_l(L_h)$	$z_r(L_h)$	gap	eigenvalue sign
6	-0.4517	-0.4439	$7.8 \times 10^{-3}$	-
8	-0.3004	-0.2999	$5 \times 10^{-4}$	-
10	-0.23987	-0.23983	$4 \times 10^{-5}$	-
	-0.6933	-0.6868	$6.6 \times 10^{-3}$	+
12	-0.2079551	-0.2079504	$4.6 \times 10^{-6}$	-
	-0.46977	-0.46908	$6.9 \times 10^{-4}$	+
14	-0.18864888	-0.8864835	$5.3 \times 10^{-7}$	-
	-0.362749	-0.362722	$2.7 \times 10^{-5}$	+
	-0.85376	-0.85315	$6.1 \times 10^{-4}$	-
16	-0.175819604	-0.175819540	$6.4 \times 10^{-8}$	-
	-0.3024077	-0.3024052	$2.5 \times 10^{-6}$	+
	-0.61069	-0.61049	$2.0 \times 10^{-4}$	-

## Behavior of gaps

1. As  $L_h \rightarrow \infty$  the gaps in  $T_C(z; L_h)$  and  $T_F(z; L_h)$  approach each other.
2. The number of gaps increases linearly and smoothly fill the entire segment  $-1 \leq z \leq z_d$  as  $L_h \rightarrow \infty$ .
3. The width of the gaps decrease (exponentially ?) as the gap location moves to the right.
4. The size of all gaps decrease (exponentially ?) as  $L_h \rightarrow \infty$ .
5. We conjecture that as  $L_h \rightarrow \infty$  the gaps form a dense set of measure zero.



## Glitches and instability for hard squares

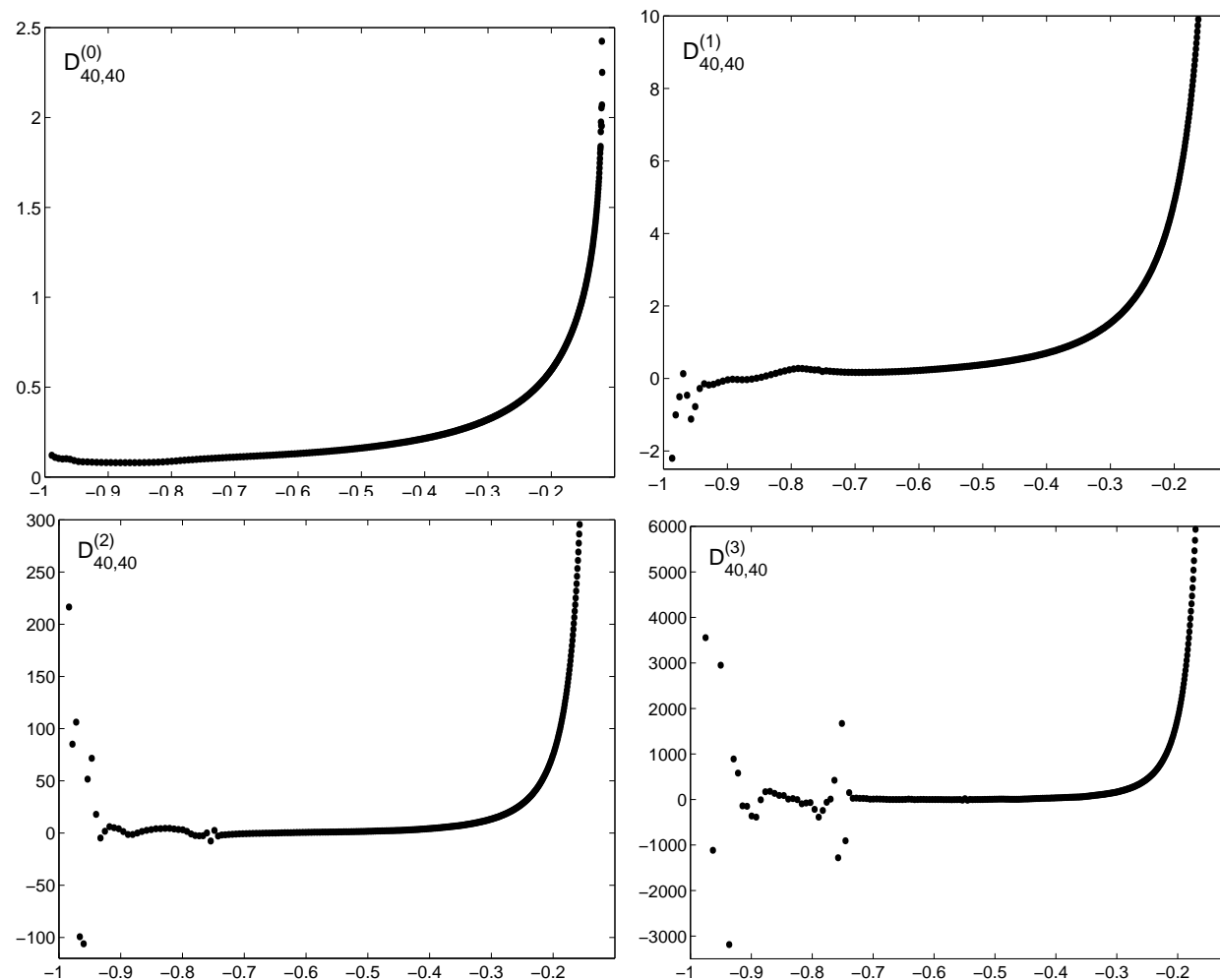
The density of zeros for hard hexagons is smooth and featureless for hard hexagons. However, for hard squares:

1. The gaps in the equimodular curves gives gaps in the density of zeros in the  $L_h \rightarrow \infty$  limit and this persists in the zeros of the  $L \times L$  lattices in deviations from smooth behavior which we term glitches.

There is increasing instability in the derivatives starting at  $z = -1$  and moving to the right as the order increases.

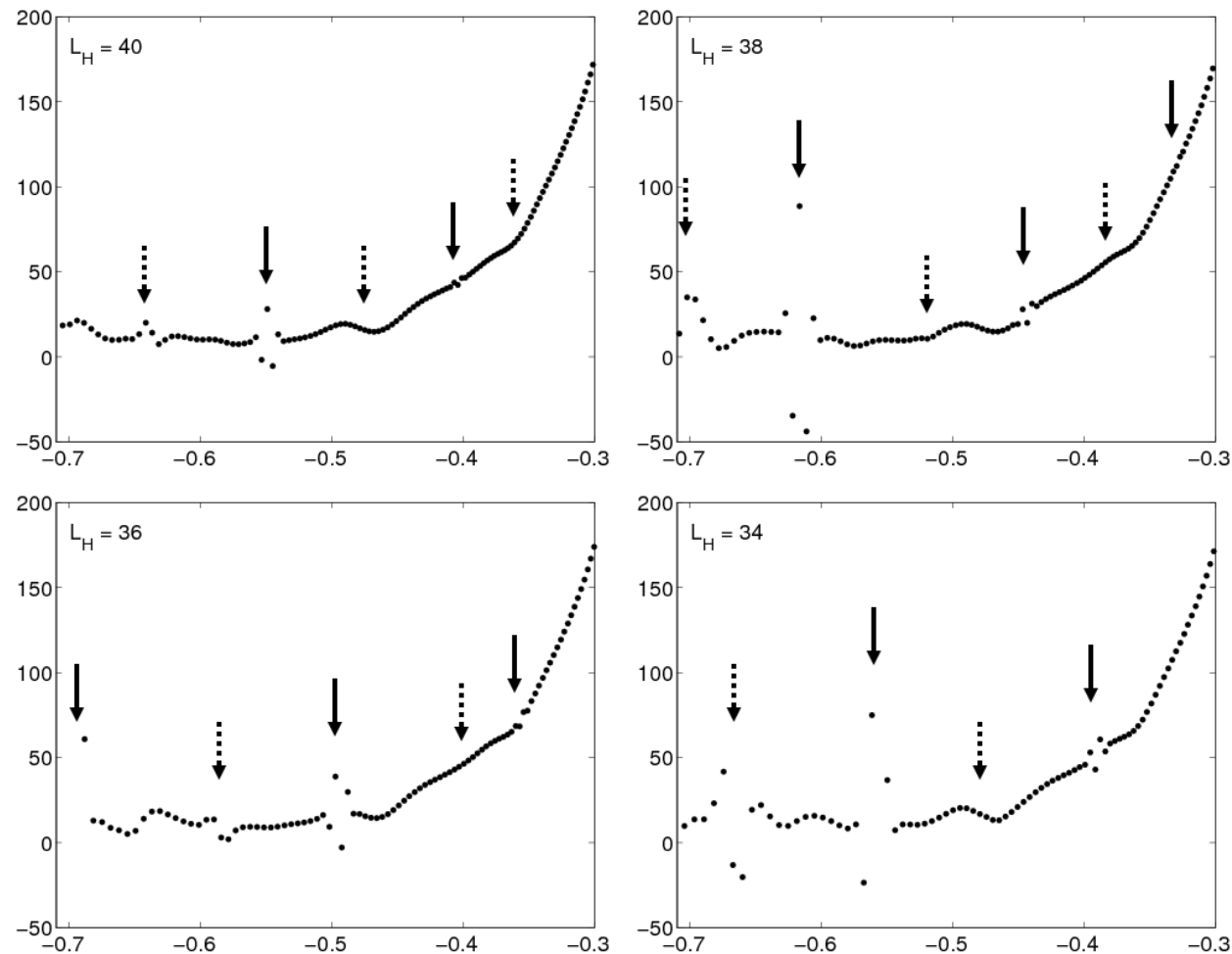
## Density and its first 3 derivatives for the $40 \times 40$ lattice

A glitch corresponding to a gap at  $z = -0.752$  is clearly seen in the second and third derivative.



## Third derivatives for $L \times L$ lattices.

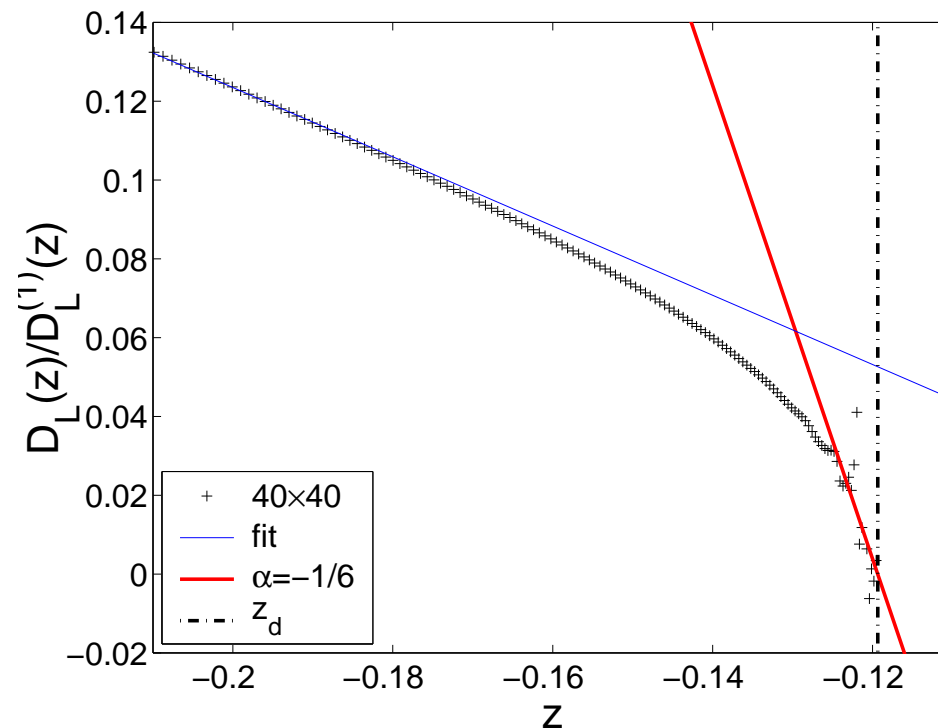
The solid arrows indicate positions of gaps where the eigenvalue phase is  $0, \pi$ . At the dotted arrows the phase is  $\pm\pi/2$ .



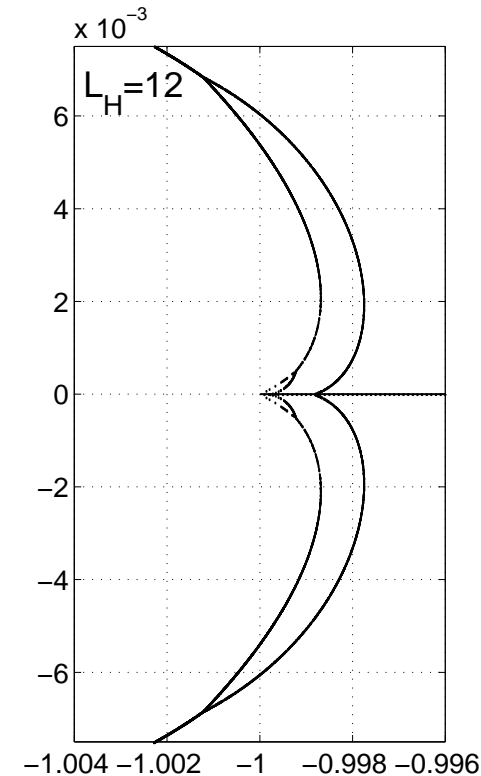
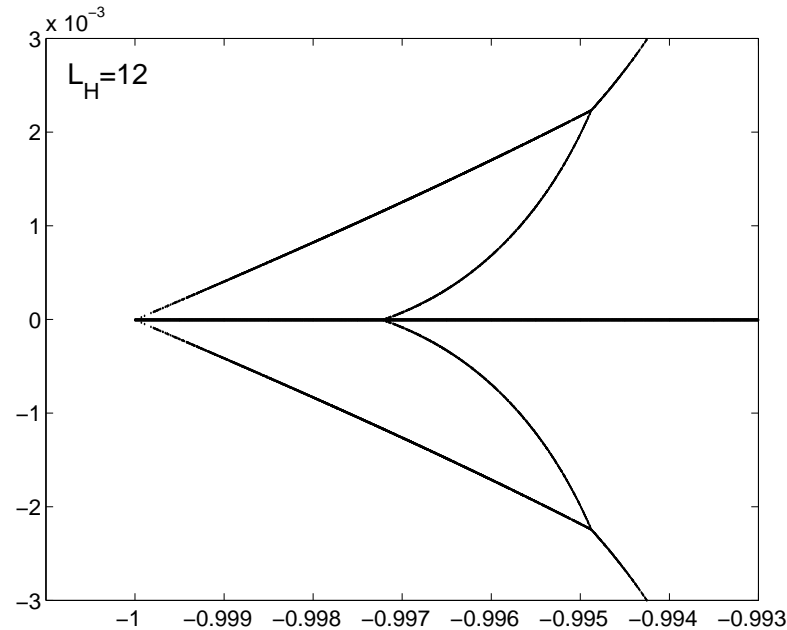
## Density of zeros as $z \rightarrow z_d$

As  $z \rightarrow z_d$  the density diverges as  $D(z) \sim (z_d - z)^{-\alpha}$ .

We plot  $D_L(z)/D_L^{(1)}(z)$  for  $L = 40$  and compare this with  $D(z)/D'(z) \sim (z_d - z)/\alpha$  with  $\alpha = 1/6$  and a fitting function  $f(z) = (z_f - z)/\alpha_f$  with  $z_f = -0.058$ ,  $\alpha_f = 1/0.88$ .



## Equimodular curves near $z = -1$



Plots in the complex fugacity plane  $z$  near  $z = -1$  for  $L_h = 12$  of the equimodular curves of hard square transfer matrix  $T_C(z; L_h)$  with  $P = 0^+$  (on the left) and  $T_F(z, L_h)$  with  $+$  parity (on the right) on a scale which shows the level crossings on the  $z$  axis.

# 5. Universality and analyticity

$z$  near  $z_d$

At  $t = z - z_d \rightarrow 0$  the free energy of hard hexagons is given as  $F = \sum_{n=0}^5 t^{n5/6} S_n(t)$  where  $S_n(t) = \sum_{k=0}^{\infty} t^k a_{k;n}$  are convergent.

Non-integrable hard squares at  $z_d$  and (and indeed, the Lee-Yang edge at  $z_{LY}$ ) are in the same universality class as hard hexagons and universality predicts that as  $z \rightarrow z_d$  hard squares will have the same 5 exponents as hard hexagons.

Does universality imply that not only will the exponents be the same as  $z \rightarrow z_d$  but that the analyticity of hard squares be the same as the analyticity of hard hexagons in a neighborhood of  $z_d$ ?

## Possible scenarios

The simplest way analyticity of hard squares can differ from hard hexagons is if the series  $S_n(t)$  fail to converge. This can happen if  $z_d$  no longer is an isolated algebraic singularity. This is what happens for the natural boundary of the Ising susceptibility. There are several features of the zeros of hard squares which differ qualitatively from hard hexagons which need to be investigated.

1. Can the gaps in the equimodular curves and glitches in the partition function zeros affect the analyticity for  $z \leq z_d$  or do their effects vanish in the thermodynamic limit?
2. Can the instabilities seen in the density of zeros near  $z = -1$  affect the analyticity ?

## Analyticity near $z = z_c$

Near  $z_c$  the zeros of hard hexagons lie on a one dimensional curve. The zeros of hard squares appear to form a wedge at  $z_c$ . Can this be made quantitatively precise and if this is the case can it affect the analyticity of of hard squares?

The simplest modification would be to allow terms of the form

$$(z_c - z)^{n_1} \ln^{n_2}(z_c - z)$$

with  $n_1$  and  $n_2$  integers. This also happens for the Ising susceptibility.



## Further questions

1. Why do hard hexagons have a necklace?
2. What is the motion of the right endpoints of the hard hexagon necklace as  $L \rightarrow \infty$ ? Can they reach  $z_c$ ?
3. Do the zeros in the hard hexagon necklace fill up an area for  $L \rightarrow \infty$ ?
4. What (if any) restrictions are put on a critical point if it is an endpoint or pinching of a line, as opposed to a wedge, of zeros?
5. Are any of these considerations relevant to the natural boundary in the Ising susceptibility?

## 6. Conclusion

Theorem:

You cannot understand a paper until you generalize it.

Corollary:

No author understands his/her most recent paper.

This talk is well explained by this corollary.